Laboratory measurements anomalous 0.1-0.5 Hz streaming potential under geochemical changes: Implications for electrotelluric precursors to earthquakes

Laurence Jouniaux and Jean-Pierre Pozzi

Laboratoire de Géologie de l'École Normale Supérieure, Centre National de la Recherche Scientifique, Paris, France

Abstract. Streaming potentials resulting from flow of various salt solutions in rock were measured on saturated sediments (Fontainebleau sandstones). The streaming potential ΔV was found to be proportional to the driving pore pressure ΔP. Pulses of amplitude 15-40 mV in the frequency range of 0.1 to 0.5 Hz were observed when the conductivity of the injected water was decreased and the fluid flow rate was relatively low, corresponding to a Darcian velocity of 17 to 30 cm/h. The amplitudes of these pulses are 47% to 133% of the corresponding steady components of the ΔV values. Such geochemically induced effects may possibly be responsible for the frequency signals from 0.1 to 0.5 Hz that were sometimes observed before an earthquake.

Introduction

Monitoring of electric and magnetic anomalies has been proposed as a possible means for predicting earthquakes because many authors reported observations of signals prior to earthquakes [*Myachkin et al.*, 1972; *Sobolev*, 1975; *Mizutani and Ishido*, 1976; *Corwin and Morrison*, 1977; *Varotsos and Alexopoulos*, 1984a,b; *Murakami et al.*, 1984; *Miyakoshi*, 1986; *Fujinawa and Takahashi*, 1990; *Gruszow et al.*, 1995]. *Fujinawa et al.* [1992] observed impulsive signals of duration ranging from about 1 s to several tens of seconds in the vertical geoelectric field before, during, and after a minor volcanic eruption on Izu-Oshima Island in Japan. Large increases in ULF magnetic signals were observed by *Fraser-Smith et al.* [1990] starting 3 hours before the October 18, 1989, Loma Prieta M7.1 earthquake, at 7 km from the epicenter. However, no significant ULF magnetic field signals were observed far from the epicenter (at 81 km) when the M6.7 Northridge earthquake occurred on January 17, 1994 [*Fraser-Smith et al.*, 1994]. ELF (10 Hz to 15 kHz) electromagnetic signals at frequencies below 450 Hz were recorded by low-altitude satellites passing over the Spitak Armenian region and anomalies were observed less than 3 hours before the strong aftershocks of the December 7, 1988, Spitak M6.7 earthquake [*Serebryakova et al.*, 1992]. Comparative analysis between observations near Loma Prieta and near Spitak were performed by *Molchanov et al.* [1992].

The steady (or dc) component of electric or magnetic anomalous signals may possibly be attributed to electrokinetic effects of fluid. *Corwin and Morrison* [1977] thought that the anomalous signal they observed was produced by a fluid flowing into a dilatant region prior to an earthquake. *Mizutani and Ishido* [1976] invoked electrokinetic effects to explain their observed signals of 5 to 10 nT. The electrokinetic effects may be produced by fluid percolation in the crust, driven by a pore pressure gradient related to precursory deformation. This model was first proposed by *Mizutani et al.* [1976], who assumed that

dilatancy prior to earthquakes [*Nur*, 1972; *Scholz et al.*, 1973] enhances the permeability of the medium and allows the fluid to flow in the vicinity of the fault. *Dobrovolsky et al.* [1989] proposed that a long-distance elastic effect induced a fluid flow and an electrokinetic effect near the electrodes of measurement. *Bernard* [1992] proposed that the electric anomalies measured far from an epicenter could be an electrokinetic signal induced by the triggering of fluid instabilities at the measurement site responding nonlinearly to precursory strain.

Miyakoshi [1986] concluded that their observation of anomalous electric signals in Japan was due to the change of the self-potential of the fractured fault rock in which one electrode was fixed, the other electrode being at a constant potential serving as a reference. He noted that fluid was flowing through the Yamasaki fault, but did not attribute this anomaly to changes in the water migration through the fault, based on consideration of the time constant of the anomaly. Another interpretation for electric and magnetic signals was given by *Jouniaux and Pozzi* [1995a] on the basis of laboratory measurements: The electrokinetic coupling coefficient of the rock near the electrode could be changed before earthquakes because the zeta potential is enhanced by fracturing, when stresses rise to over 75% of the yield stress that ruptures the seismic zone. This increse in zeta potential could lead to an electrokinetic potential anomaly [*Jouniaux and Pozzi*, 1995a]. *Draganov et al.* [1991] suggested that the magnetic anomalies observed at the Earth's surface before the Loma Prieta earthquake [*Fraser-Smith et al.*, 1990] were the results of magnetic fields induced by fluid flow of conductivity 4 S/m and velocity 4 cm/s at a seismogenic depth of 5 km. However, such conditions are not likely to be met as noted by *Fenoglio et al.* [1995].

The oscillatory nature of the signals observed by *Fraser-Smith et al.* [1990] has been attributed by *Fenoglio et al.* [1995] to an electrokinetic effect associated with unsteady fluid flow during failure of faults. *Fenoglio et al.* [1995] suggested that the stop-and-go fracture propagation associated with rapid fluid flow in a shear fracture 17 km deep could generate magnetic signals measurable at the surface as a result of electrokinetic effects.

The preceding discussion shows that many authors have invoked electrokinetic phenomena to explain electric and

magnetic anomalies observed prior to earthquakes near or far from the epicenter region. Streaming potentials refer to the electrical signals produced when a fluid flows in a porous medium and this effect can be quantified through experimental results. Few laboratory data of geophysical interest on streaming potential are available [*Ahmad*, 1964; *Somasundaran and Kulkarni*, 1973; *Ishido and Mizutani*, 1981; *Massenet and Van Ngoc*, 1985; *Morgan et al.*, 1989; *Morat et al.*, 1992; *Antraygues and Aubert*, 1993; *Jouniaux et al.*, 1994; *Pozzi and Jouniaux*, 1994; *Jouniaux and Pozzi*, 1995a,b].

We present in this paper some laboratory measurements of streaming potentials on a saturated Fontainebleau sandstone (quartz content more than 99%), using various conductivities of salt solutions. In particular, we report the observation of the occurrence of unusual signal pulses having a duration of a few seconds under the condition of changing fluid conductivity. These findings may be relevant to recent reports of changes in the geochemistry of groundwater as a precursor to earthquakes [*Tsunogai and Wakita*, 1995; *Toutain et al.*, 1997].

Electrokinetic Phenomena

Electrokinetic phenomena arise from the existence of some electrical double layers that are formed at the solid-liquid interface. The currently accepted model for the rock-fluid interface is derived largely from the work of *Stern* [1924]. The double layer is made up of a stationary layer of ions (the Helmholtz layer) adsorbed to the surfaces of the minerals comprising the rock, and a diffuse mobile layer (the Gouy-Chapman zone) on the aqueous side of this interface that extends into the liquid phase (for detailed description, see *Adamson* [1976], *Dukhin and Derjaguin* [1974], and Hunter [1981]).

When a fluid is made to flow through a porous medium, there will be an occurrence of a potential, the so-called streaming potential, across the sample in the flow direction because of the relative motion between the solid and the liquid. On the closest plane to the surface on which fluid motion takes place, the potential is defined as the ζ potential, which is the potential that is manifested in streaming-potential measurements. Streaming potentials generated by fluids moving through porous media or capillaries are governed by the Helmholtz-Smoluchowski equation as discussed below [*Overbeek*, 1952; *Nourbehecht*, 1963]. In a porous medium the electric current density I (A/m^2) and the fluid flow J (m/s) are coupled according to the following equations:

$$-I = \frac{\sigma_f}{F} \text{grad} V - \frac{\varepsilon\zeta}{\eta F^o} \text{grad} P \qquad (1)$$

$$-J = -\frac{\varepsilon\zeta}{\eta F^o} \text{grad} V + \frac{k}{\eta} \text{grad} P \qquad (2)$$

where V is the electric potential, P is the fluid pressure, σ_f and ε are the electrical conductivity and the dielectric constant of the fluid, ζ is the zeta potential, η the dynamic viscosity of the fluid, k is the permeability of the porous medium. F^o is the formation factor ($\sigma_{fluid}/\sigma_{rock}$, ratio between fluid and rock conductivities) with a very high fluid conductivity (typically, 0.1 S/m for a lot of rocks [see *Ruffet*, 1993]) when surface conduction is absent, and F is the formation factor for the fluid conductivity being studied (i.e., possibly with surface conductivity). The first term on the right-hand side in (1) represents Ohm's law, and the second term in (2) represents Darcy's law. In a steady state equilibrium the

convection current (due to grad P) is balanced by the conduction current (due to grad V). Equating these currents leads to the ratio $\Delta V/\Delta P$ called the streaming-potential cross-coupling coefficient C_s, or simply, the coupling coefficient:

$$C_s = \frac{\Delta V}{\Delta P} = \frac{\varepsilon\zeta}{\eta\sigma_f}\frac{F}{F^o} \qquad (3)$$

which is the Helmholtz-Smoluchowski equation [*Dukhin and Derjaguin*, 1974]. The above equations are given here because they are found in different forms in the *literature [Ishido and Mizutani*, 1981; *Morgan et al.*, 1989; *Pride*, 1994]. ΔV is the generated potential, and ΔP is the applied pore-pressure difference. For a complete development of the equations governing the coupled electromagnetics and acoustics of the porous media, see *Pride* [1994]; for further details on surface conductivity, see *Revil et al.* [1996]. Equation (3) implies that the currents are of equal magnitude and opposite flow along the same path. When surface conductivity is negligible, $F=F^o$, and we have

$$C_s = \varepsilon\zeta/\eta\sigma_f \qquad (4)$$

Double Layer For Quartz-Water Systems

The streaming potential is due to the motion of the diffuse layer induced by the applied fluid pressure gradient along the interface. The double layer for quartz-water systems is described here from a chemical point of view.

Population Distribution of Sites at Quartz-Water Interface

Dove and Elston [1992] quantified the distribution of surface species on pure quartz in a solution of several values of sodium concentration and pH (at 25°C). For a quartz surface in pure water the authors calculated how sites at the mineral surface are distributed at pH 5. Note that at pH 5 the activity of H_3O^- ions is 10^{-5} which is 10^4 times greater than the activity of OH^- ions (10^{-9}). *Dove and Elston* [1992] noted that an increase in sodium concentration of the bulk solution redistributes the population balance of surface complexes in favor of more SiO^- and $SiONa^+$. However, their predictions for a solution of 10^{-4} M NaCl and pH 5 showed a predominant site fraction SiOH of 99.85% and a site fraction SiO^- of 0.15%. A more concentrated solution of 0.2 M NaCl still shows that surface sites are dominated by SiOH (99.52%) with a site fraction of SiO^- and SiONa of only 0.43% and 0.05%, respectively. These estimates indicate that all of the experiments conducted in the present study had surfaces which were dominated by more than 99% of the neutral complex and which had negative deprotonated complex SiO^-. As a consequence, the cations of electrolyte solutions are electrostatically attracted to this negative surface and anions are repulsed.

Species That Can Form at Quartz-Water Interface

The hydrated counterions Na^+ present in the diffuse layer are thought to be maintained at some distance from the rock surface by the hydratation water around each cation and the water adsorbed on the surface. The outer Helmholtz plane defines the closest distance approached by the hydrated counterions Na^+ at which distance the potential is Φ_k. Note that there is an excess of cations in the diffuse layer. Strongly adsorbed ions such as

hydrogen interact closely with unsaturated oxygens in the innermost layer.

Position and State of the Species at Quartz-Water Interface

The exact position of the shear plane at a quartz-water interface is not clear. A common assumption is that zeta potential is identical to Φ_s, meaning that the hydraulic flow shears the diffuse layer up to the surface, the first layer of counterions that constitute the Helmholtz layer being mobile. This assumption would be justified at low ionic strengths (10^{-4} and 10^{-3} M) and at pH values below 9 [Li and De Bruyn, 1966]. The motion of the diffuse layer induced by the applied pore pressure is carrying an excess of hydrated Na^+ ions and H_3O^- ions. Therefore an excess of positive charge exists at one end of the sample where the fluid pressure is the smallest whereas a deficit in positive charges exists at the other end of the sample where the fluid pressure is the highest. As a result the electrokinetic coupling coefficient $\Delta V/\Delta P$ is negative, leading to a negative zeta potential.

The effect of pH on zeta potential is well known: the negative zeta potential can increase and become zero and may even be positive. The isoelectric point is the pH for which the zeta potential is zero. Li and De Bruyn [1966] showed from electrokinetic measurements of NaCl solutions on pure quartz an isoelectric point at pH value lower than 2. Sharma et al. [1987] showed from measurements on baked and unbaked sandstone oxide and Ottawa sand with NaCl solution of 10^{-2} and 10^{-3} M at 25°C that the isoelectric point was between 2 and 3.5. Ishido and Mizutani [1981] measured an isoelectric point at pH 2 for quartz in solution of 10^{-3} N KNO_3. Therefore the zeta potential is expected to be negative for pH values above 2-3.5.

Experimental Procedure

Our experiments were conducted using Fontainebleau sandstone composed of more than 99% pure quartz with grain size of about 250 μm. In a previous study [Jouniaux and Pozzi, 1995a] we showed that the formation factor F° was 91, the porosity 11%, and the permeability 6.5×10^{-14} m^2 (65 mD). Measurements were made on sample F313 using a pressure cell described by Jouniaux and Pozzi [1995a]. The sample was cut into a cylinder 50 mm long and 25 mm in diameter. The sample was subsequently dried at 70°C in vacuum for 8 hours. Then it was saturated with distilled water of resistivity 2×10^3 Ωm.

The first set of measurements (Figures 1 and 2) were performed when the sample was subjected to a quasi-hydrostatic pressure such that the axial stress was 12±0.5 MPa and confining pressure was 11±0.1 MPa. The press is servocontrolled in displacement; thus the strain was constant. The streaming potential was measured using different NaCl concentrations, starting with distilled water of pH 5, which had a resistivity of 1030 Ωm, up to a concentration of 9×10^{-4} mol/L, which had a resistivity of 103 Ωm. The intermediate solutions had resistivities of 720 Ωm and 490 Ωm.
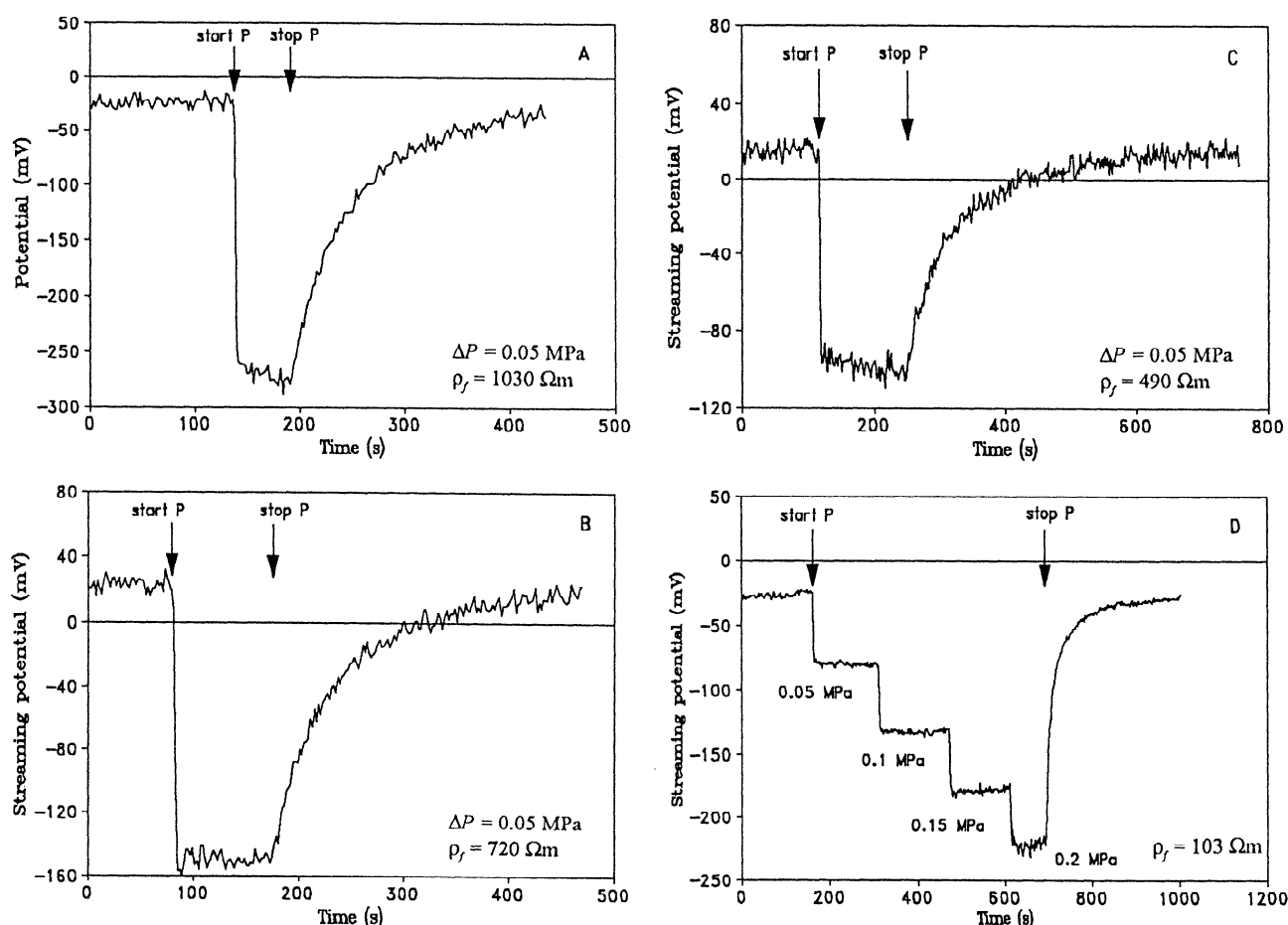
Figure 1. Examples of measured streaming potential (ΔV) when a pore pressure difference ΔP is applied from "start P" to "stop P" for four fluids of different resistivity ρ_f.
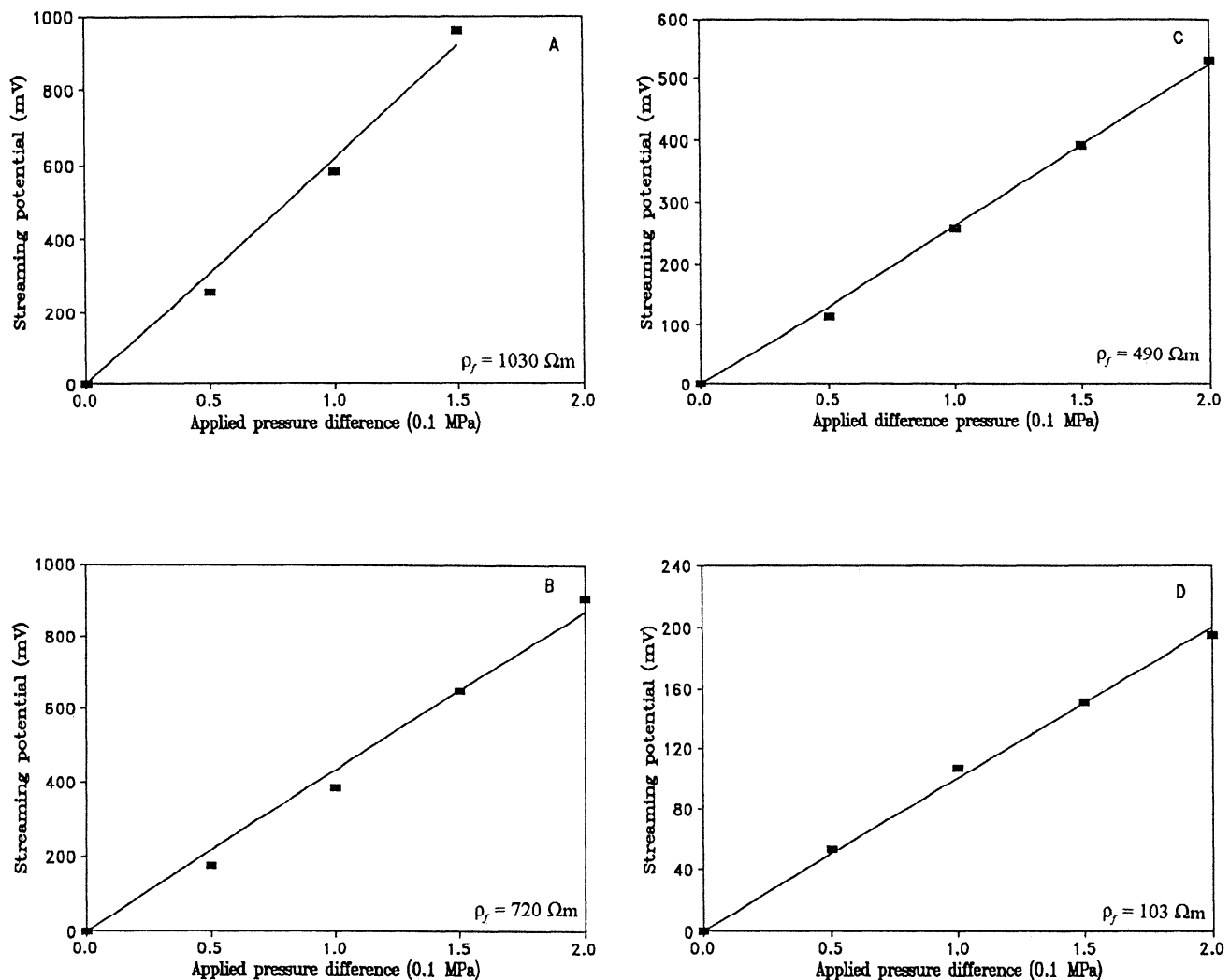
Figure 2. Measured streaming-potential values (in absolute value) versus applied pore pressure difference ΔP for the four fluids corresponding to those of Figure 1.

After these measurements with salt solutions, measurements with distilled water were performed, leading to transient streaming potentials (Figure 3). These measurements were performed during the beginning of a deformation cycle, when the axial stress and confining pressure were 10 ± 1 MPa and 10.0 ± 0.1 MPa, 24.5 ± 0.5 MPa and 10.7 ± 0.1 MPa, 67 ± 2 MPa and 11.3 ± 0.1 MPa, 118 ± 2 MPa and 11.3 ± 0.1 MPa, respectively, for the four measurements shown in Figure 3. The sample strength was 262 MPa.

The electrodes used in our experiment are made of beryllium-bronze with a 3 mm hole at the center and two linked circular grooves allowing the fluid to flow uniformly in the axial direction through the sample. The upper and lower electrodes are isolated from the conductive press and the cell by an insulating alumina piston and an insulating pastille, respectively. The dielectric constant of the fluid ε_{H2O} is 7.04-7.18 $\times 10^{-10}$ F/m at temperatures between 17°C and 24°C.

Resistivity Measurement

The resistance of the sample was measured with an HP 4284A impedance meter at a frequency of 4 kHz [Ruffet et al., 1991] as for all previous measurements. The fluid in the cylindrical hole

of the insulating piston and the insulating pastille is in contact with the sample [Jouniaux and Pozzi, 1995a] and can provide a conduction path outside of the sample. The resistance R_w of this exterior conduction path which was measured is in parallel with the conduction path through the sample. The effective resistance between the electrodes R_m is

$$1 / R_m = (1 / R_s) + (1 / R_w) \tag{5}$$

where R_s is the resistance of the sample. The resistivity ρ_w of the fluid which was used for the calculation of R_w, was measured after the fluid flowed out of the cell and as soon as the flow was stopped by using a conductivity cell. This procedure allows us to use the resistivity of the sample (ρ_s) and the resistivity of the fluid (ρ_w) to approximately represent the values that were present during the streaming-potential measurement.

Streaming Potential Measurement

The streaming potential was measured during fluid flow by an HP 34401A voltmeter with an input resistance of more than 10^{10} Ω. The resistance of the water in the insulating piston (R_w) is taken into account. In this case the total electrical current is
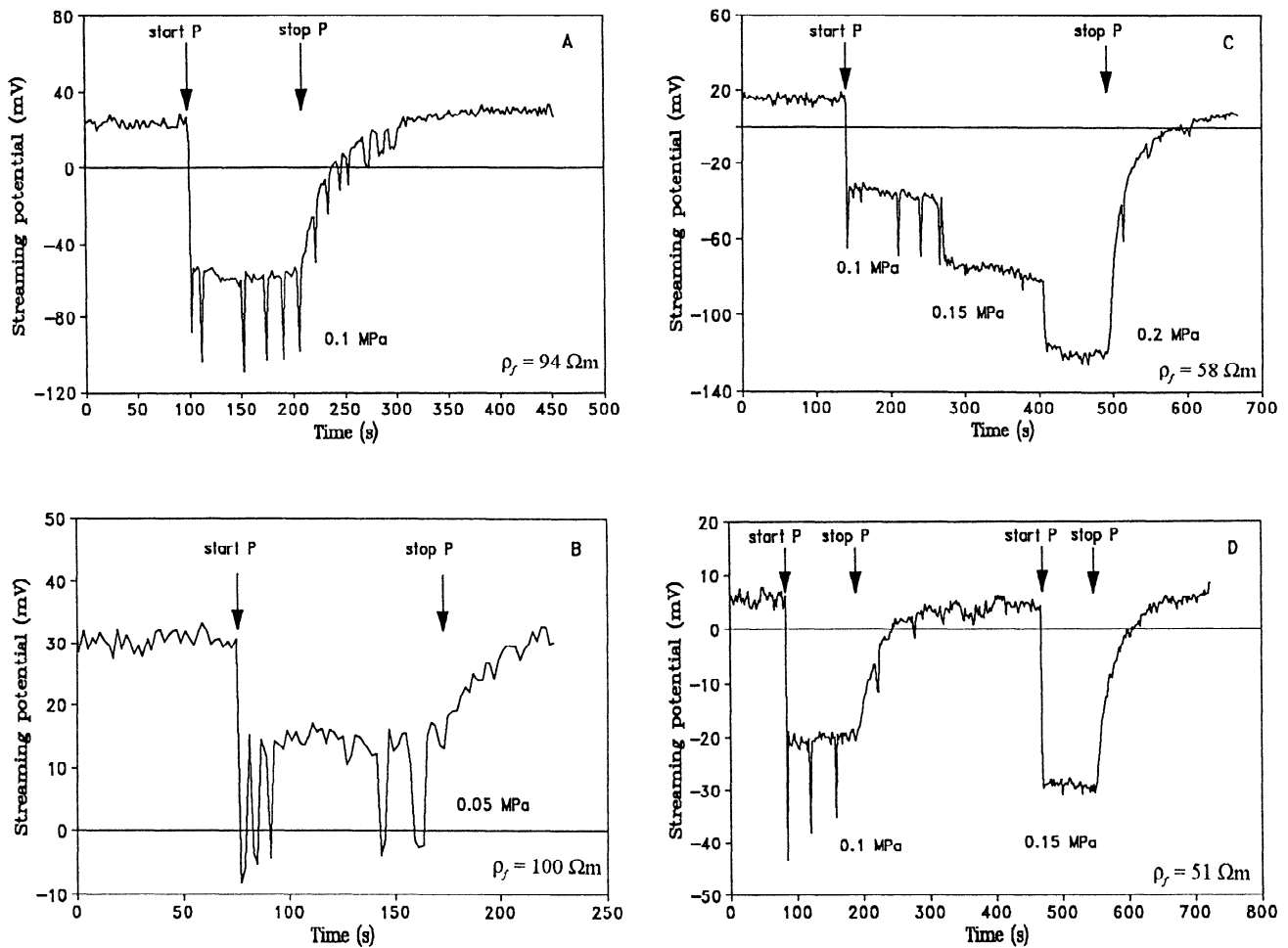
Figures 3. Streaming-potential measurements for different fluid resistivities (a) 94 Ωm, (b) 100 Ωm, (c) 58 Ωm and (d) 51 Ωm. The 0.1-0.5 Hz pulses were observed only for low fluid flow rate when $\Delta P = 0.05$ or 0.1 MPa and when the injected water was less conductive than the previous solution. The electrokinetic coupling coefficients are (a) -85 mV/0.1 MPa, (b) -30 mV/0.1 MPa, (c) -61 mV/0.1 MPa, and (d) -24 mV/0.1 MPa.

no longer zero in the sample. Under this condition, (3) may be modified as follows:

$$\frac{\Delta V}{\Delta P} = C_s / (1 + \frac{R_s}{R_w})$$ (1')

C_s being the electrokinetic coupling coefficient that would have been measured without this leakage current outside the sample (when $R_w \gg R_s$). Data were recorded, once per second, with a PC computer and an IEEE interface. The different fluids were made to flow through the sample from the most resistive to the least until the measured resistivity of the fluids flowing out of the sample was constant. We then began the streaming-potential measurements. The confining pressure was applied manually by a pump. The pore pressure difference ΔP was applied by using a pump and measured by using a manometer. The pump is manually controlled; typical error in a measured pressure difference of 0.1 MPa is ±0.01 MPa for the F313 sample. The applied pore pressure difference was kept constant usually for 50 to 200 s. Fluid flow rate and fluid resistivity were measured during streaming-potential measurement, and the values given are average for the 50-200 s durations.

Results

We first describe the steady state streaming-potential measurements and then focus on pulses of 2-9 s duration that were observed when the input solution was replaced by a less conductive one and when the water flow was relatively low.

Steady State Streaming Potential Measurements

A typical streaming-potential variation when a pressure difference of 0.05 MPa was applied is shown in Figure 1a for a solution which is distilled water having a resistivity of 1030 Ωm. The potential was -25 mV when the fluid was not flowing through the sample and dropped to about -275 mV when the pressure was applied. The streaming potential is therefore -250 mV. Similar measurements were performed with pressure differences of 0.1 MPa and 0.15 MPa. The streaming potential is shown to be proportional to the applied pore pressure (Figure 2a). From the slope of the best fit line in Figure 2a, we obtain an apparent electrokinetic coupling coefficient $\Delta V/\Delta P$ of -614 mV/0.1 MPa, and a corrected coefficient C_s of -1331 mV/0.1 MPa after taking into account the resistance of the fluid in the

cylindrical hole of the piston (R_w) (1'). The linearity between the streaming potential and the applied pore pressure is an important result and is not accepted by all investigators [*Middleton*, 1996].

When a more conductive salt solution of resistivity 720 Ωm (corresponding to a concentration of NaCl of 1.5×10^{-4} mol/L) was used under a pore pressure difference of 0.05 MPa, the streaming potential was -175 mV (Figure 1b). The streaming potentials for four different pore pressure differences are shown in Figure 2b, which gives a $\Delta V / \Delta P$ coefficient of -435 mV/0.1 MPa, and a C_s coefficient of -734 mV/0.1 MPa. Similar results for a salt solution of resistivity 490 Ωm corresponding to a NaCl concentration of 2×10^{-4} mol/L are shown in Figures 1c and 2c. The coefficient C_s is -404 mV/0.1 MPa. The results for the salt solution of resistivity 103 Ωm corresponding to a NaCl concentration of 9×10^{-4} mol/L are shown in Figures 1d and 2d. When the fluid is not flowing through the sample, the electric potential was -25 mV, it dropped to -78 mV when ΔP was 0.05 MPa, -132 mV when ΔP was 0.1 MPa, -176 mV when ΔP was 0.15 MPa and -220 mV when ΔP was 0.2 MPa. These measurements lead to a C_s coefficient of -157 mV/0.1 MPa.

When using more conductive fluid of resistivity 11 Ωm (9.5×10^{-3} mol/L of NaCl), 1.1 Ωm (0.1 mol/L), or 0.11 Ωm (1.45 mol/L of NaCl), the streaming potential was no longer constant for a constant applied pore pressure. The potential for the most conductive solution was too small to measure. Table 1 summarizes the electrokinetic coupling coefficient (C_s in mV/0.1 MPa) for the four solutions.

Transient streaming potential measurements

Distilled water of *p*H 5 and resistivity 3×10^3 Ωm was made to flow through the sample seven days (time needed to process the previous data) after the above-mentioned measurements. The solution flowing out of the cell became 30 times more conductive than the injected water with a resistivity of about 100 Ωm, still 10^3 less conductive than the most conductive solution used earlier (0.1 Ωm). Streaming potential was measured when the fluid resistivity became constant. Fluid flow rate through the sample was about 2.4×10^{-8} m^3/s when $\Delta P = 0.05$ MPa and 4.2×10^{-8} m^3/s when $\Delta P = 0.1$ MPa. Since the pore volume of the sample is 2.7×10^{-6} m^3, the residence time of fluid in the sample is about 2 min when $\Delta P = 0.05$ MPa, and 1 min when $\Delta P = 0.1$ MPa. As the exchange rate for sodium ions is of the order of 10^{-9} s, we assumed that the fluid conductivity inside the sample is the same as that measured after the fluid flowed through the sample. The measured permeability was 4.9×10^{-14} m^2, showing a 25% decrease compared to value measured just before the above-mentioned measurements with salt solutions (6.5×10^{-14} m^2; see *Jouniaux and Pozzi* [1995a] for the method). In all the experiments described below the injected fluid was distilled water. The electrokinetic coupling coefficient C_s is equal to the measured electrokinetic coupling coefficient $\Delta V / \Delta P$ as the resistance R_w of the exterior conduction path is important compared to the resistance of the sample R_s. Indeed the insulating piston is full of distilled water whereas it was full of salt water for the previous measurements (the resistance R_w is 49.4 MΩ, while the resistance of the sample is in the range 303-618 kΩ).

Table 1. Electrokinetic Coupling Coefficients C_s for Various Solutions of Resistivity ρ_f

| NaCl, mol/L	Pure Water	1.5×10^{-4}	2×10^{-4}	9×10^{-4}
ρ_f, Ωm	1030	720	490	103
C_s, mV/0.1 MPa	-1331	-734	-404	-157

Table 2. Electrokinetic Coupling Coefficient C_s and 0.1-0.5 Hz Pulse Amplitude

ρ_f, Ωm	94	100	60	51
C_s, mV/0.1 MPa	-85	-30	-30	-24
Pulse amplitude, mV	40	20	30	15-25

As shown in Figure 3a when a pressure difference of 0.1 MPa was applied, the potential decreases from 25 mV to about -60 mV. After flowing through the sample, the solution has a resistivity of 94±1 Ωm. The electrokinetic coupling still defined from the dc component, is -85±20 mV/0.1 MPa. Superimposed on the dc signal are some 40 mV pulses with a duration of 2-6 s. In another experiment the resistivity of the fluid was 100±5 Ωm after flowing through the sample. The potential decreased from 30 mV to 15 mV when the applied pressure difference was 0.05 MPa. The electrokinetic coupling coefficient deduced from this measurement is -30±9 mV/0.1 MPa. Again pulses of amplitude 20 mV and duration of 4.5-9 s were observed (Figure 3b). Other measurements with various applied pressure differences are shown in Figures 3c and 3d. Such pulses were seen when the applied pressure difference was 0.1 MPa but not seen for larger applied pressure differences (0.15 MPa and 0.2 MPa). The fluid resistivity after flowing through the sample is 58±8 Ωm in Figure 3c and 51±5 Ωm in Figure 3d. The electrokinetic coupling coefficients deduced from these measurements are -61±5 mV/0.1 MPa and -24±5 mV/0.1 MPa in Figures 3c and 3d, respectively. The amplitudes of the pulses are about 15 to 25 mV and the duration 2-8 s. Table 2 summarizes the electrokinetic coupling coefficient (C_s in mV/0.1 MPa) and pulses corresponding to the different solution resistivities (ρ_f in Ωm).

Discussion

From the above-mentioned steady state measurements reported previously [*Jouniaux and Pozzi*, 1995a], the streaming potential is roughly proportional to the fluid resistivity with a slope of 1.2 mV/0.1 MPa/Ωm (Figure 4). This result leads to a roughly estimated zeta potential of -17 mV, using (4) with the assumptions that $F = F^\circ$ and ε and η are constant. Note that zeta potential depends on salt concentration [*Pride and Morgan*, 1991] and that ε is of the order of 2-3 $\times 10^{-10}$ F/m for salt solutions. For all concentrations used, the surface species on sandstones are expected to be 99% SiOH as discussed in the description of the quartz-water systems. Since solutions of *p*H 5
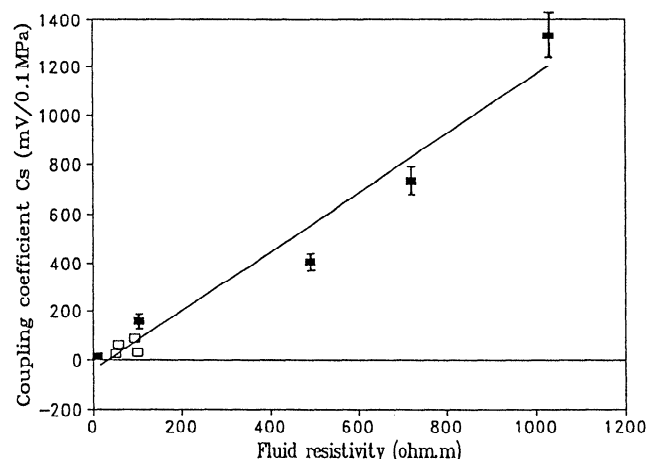
Figure 4. Electrokinetic coupling coefficient (mV/0.1 MPa) versus fluid resistivity obtained from steady state (solid squares) and transient (open squares) measurements.

are used in our study, a negative zeta potential is consistent with the studies on the isoelectric point.

The electrokinetic coupling coefficient based on the transient streaming potential measurements (open squares in Figure 4) is qualititavely consistent with the steady state measurements made previously (solid squares in Figure 4).

Note that the transient streaming-potential pulses were observed only (1) when the injected fluid is less conductive than the previous solution by a factor 10^3, and (2) when the applied pressure difference is as small as 0.05 MPa or 0.1 MPa, corresponding to a Darcian velocity of 17 cm/h (4 m/d) to 30 cm/h (7.4 m/d). The amplitudes of these pulses are about 15 to 40 mV, which represent 47%, 133%, 60%, and 60 to 100% of the measured signals in the examples shown in Figures 3a, 3b, 3c, and 3d, respectively. Note that for each measurement the fluid resistivity is approximately constant (with some fluctuations as shown by the error bars) and did not change sufficiently to induce the observed pulses. A variation of 50% in water resistivity, for example, would induce a variation of 50% in streaming potential as C_s is proportional to the fluid resistivity (3). Moreover in all the streaming-potential measurements performed in our laboratory, usually on sandstone and limestone samples, pulses in the measurements were only observed when less conductive water was made to flow through a previously salted sample. The opposite arrangement, when a more conductive water was made to flow through the sample, never produced such pulses.

The appearance of the pulses suggests that more H_3O^- cations and hydrated counterions Na^+ of the diffuse layer are suddenly carried along by the fluid. These charges may have resulted from the salt deposited in the rock, part of which is put into the solution when the distilled water is used. Indeed the decrease in the permeability by 1/4 between the first measurement and the measurements performed 7 days later shows that some salt deposit very likely exists on the surface of the rock. If certain heterogeneity of salt deposit on the surface of the rock could explain some sudden increase of carried cations (hydrated ions Na^+) it cannot explain the frequency of these pulses (0.1 to 0.5 Hz) because the exchange rate for sodium ion is of the order of 10^{-9} s. Since all our measurements were performed on the sample subjected to stresses below the rupture (strength less than 45%), we do not think that microcracks could give rise to these pulses. Moreover no such pulses were observed when the sample was stressed from 50% of the strength up to rupture. In view of electrokinetic coupling coefficient given by (3) not being dependent on sample size, we think that these pulses are not related to sample size and similar pulses can be observed in geophysical field experiments.

In our opinion, these pulses may arise from random or transient breaks of fluid through pore throats the size of which have been reduced by salt deposits. This suggestion is consistent with the observation that the pulses disappeared at higher pressure difference (salt deposit has been swept away from the pore throats).

Possible Implications for Electrotelluric Earthquake Precursors

The streaming-potential pulses observed in our laboratory experiments can be used to explain certain oscillary electromagnetic signals observed in the field before some earthquakes.

Variations in groundwater flow before and after earthquakes have often been reported in the literature. For example, a sudden hot-spring erupted in the epicentral region several months before the 1923 Kanto $M=7.9$ earthquake [Wakita, 1982]. Water level changes of about 5 to 10 cm were reported prior to the 1976 Tangshan earthquake in China [Jin, 1985]. Along the San Andreas fault in California, changes in water levels up to 16 cm are observed to accompany some creep events [Roeloffs et al., 1989]. Abnormal increases in water flow lasting 6 to 12 months have been measured in springs and wells at distances of the order of 50 km from the epicenter, beginning a few days after some earthquakes, especially those generated along some major normal faults. Expelled water volumes were 0.2 to 0.5 km^3 for two earthquakes of magnitude 7 and 7.3 studied by Muir-Wood and King [1993].

More recently, geochemical evidence of ground-water changes were reported before earthquake [Toutain et al., 1997; Tsunogai and Wakita, 1995]. Tsunogai and Wakita [1995] reported geochemical evidence of precursory groundwater changes observed at a distance of 20 km from the epicenter of the $M=7.2$ Kobe earthquake on January 17, 1995. Chlorine ion (Cl^-) and sulfate ion (SO_4^{2-}) concentration of water from a 100 m deep well began to increase 6 months before the earthquake. Four days before the earthquake, the Cl^- concentration was about 10% higher than the average background level. Tsunogai and Wakita stated that chemical changes observed before the earthquake could be attributed to the introduction of groundwater enriched in Cl^- and SO_4^{2-} to the artesian layer of the wells and coming from the fracture zone. They suggested that changes of groundwater flow may occur by a change either in regional tectonic stress or in permeability. Increased groundwater discharge was observed in many parts of the aftershock region [King et al., 1995].

The above-mentioned examples illustrate that the chemical composition of water can be changed in places affected by earthquake-related variations of groundwater flow, though the mechanism needed to explain these changes is still uncertain [Dobrovolsky at al., 1989; Draganov et al., 1991; Bernard, 1992; Fenoglio et al., 1995]. However it is likely that water flowing in some rock layer can introduce changes in conductivity. In such cases, electrokinetic signals including pulses of duration 2-9 s may be produced by fluid flow, as suggested by our laboratory measurements. Our interpretation involves electrokinetic effects not at the source but near the site of measurements, for an electromagnetic field is easily attenuated in the conductive Earth [Honkura, 1992]. Our suggestion of fluid breaking through salt deposit pore throats is similar to the physical mechanism proposed by Fenoglio et al. [1995], which involves nonuniform fluid flow in the Earth resulting from pressure decrease due to dilatancy, partial blockage by silica deposition, and clearing of deposition as the pressure increases. The paths of fluid flow, of electric currents, and the changes in chemical composition in the Earth are, of course, more complex and could induce more complicated signals.

The dc component of streaming potential could be observed by measuring the vertical electric field, or the horizontal electric field if a lateral heterogeneity in the electrokinetic coupling coefficient values exists as suggested by Fitterman [1979]. Indeed, the vertical component should be dominant because it is proportional to the vertical driving pore pressure and to the the electrokinetic coupling coefficient (no heterogeneity in C_s is needed).

Could we explain the observation that no electric coseismic anomalies are observed for most earthquakes? Our laboratory measurements show that the pulses were observed only when the fluid flow was relatively low and when less conductive fluid was flowing through the rock. If these conditions are met, the observation of pulses of 0.1 to 0.5 Hz can be attributed to electrokinetic effects caused by groundwater flow changes before the earthquake.

Conclusion

Transient streaming-potential variations with pulses of amplitude 15-40 mV and frequency 0.1 to 0.5 Hz were observed under geochemical changes. Such geochemically induced effects may possibly be responsible for the signals of frequency 0.1 to 0.5 Hz that were sometimes observed before an earthquake.

References

Adamson, A. W., *Physical Chemistry of Surfaces*, Wiley-Interscience, New York, 1976.

Ahmad, M., A laboratory study of streaming potentials, *Geophys. Prospect.*, *12*, 49-64, 1964.

Antraygues, P., and M. Aubert, Self potential generated by two-phase flow in a porous medium: Experimental study and volcanological applications, *J. Geophys. Res.*, *98*, 22,273-22,281, 1993.

Bernard, P., Plausibility of long distance electrotelluric precursors to earthquakes, *J. Geophys. Res.*, *97*, 17,531-17,546, 1992.

Corwin, R. F., and H. F. Morrison, Self-potential variations preceding earthquakes in Central California, *Geophys. Res. Lett.*, *4*, 171-174, 1977.

Dobrovolsky, I. P., N. I. Gershenzon, and M. B. Gokhberg, Theory of electrokinetic effects occuring at the final stage in the preparation of a tectonic earthquake, *Phys. Earth Planet. Inter.*, *57*, 144-156, 1989.

Dove, P. M., and S.F. Elston, Dissolution kinetics of quartz in sodium chloride solutions: Analysis of existing data and a rate model for 25C, *Geochim. Cosmochim. Acta*, *56*, 4147-4156, 1992.

Draganov, A. B., U. S. Inan, and Yu.N. Taranenko, ULF magnetic signatures at the Earth surface due to groundwater flow: A possible precursor to earthquakes, *Geophys. Res. Lett.*, *18*, 1127-1130, 1991.

Dukhin, S. S., and B.V. Derjaguin, *Surface and Colloid Science*, vol. 7, edited by E. Matijevic, John Wiley, New York, 1974.

Fenoglio, M. A., M. J. S. Johnston, and J. D. Byerlee, Magnetic and electric fields associated with changes in high pore pressure in fault zones: Application to the Loma Prieta ULF emissions, *J. Geophys. Res.*, *100*, 12,951-12,958, 1995.

Fitterman, D. V., Theory of electrokinetic-magnetic anomalies in a faulted half-space, *J. Geophys. Res.*, *84*, 6031-6040, 1979. (Correction, *J. Geophys. Res.*, *86*, 9585-9588, 1981.)

Fraser-Smith, A.C., A. Bernardi, P.R. McGill, M.E. Ladd, R.A. Helliwelll and O.G. Villard Jr., Low-frequency magnetic field measurements near the epicenter of the Ms 7.1 Loma Prieta earthquake, *Geophys. Res. Lett.*, *17*, 1465-1468, 1990.

Fraser-Smith, A. C., P. R. McGill, R. A. Helliwell, and O.G. Villard Jr., Ultra-low frequency magnetic field measurements in southern California during the Northridge earthquake of 17 January 1994, *Geophys. Res. Lett.*, *21*, 2195-2198, 1994.

Fujinawa, Y., and K. Takahashi, Emission of electromagnetic radiation preceding the Ito seismic swarm of 1989, *Nature*, *347*, 376-378, 1990.

Fujinawa, Y., T. Kumagai, and K. Takahashi, A study of anomalous underground electric field variations associated with a volcanic eruption, *Geophys. Res. Lett.*, *19*, 9-12, 1992.

Gruszow, S., J. C. Rossignol, C. Pambrun, A. Tzanis, and J.L. Le Mouël, Characterisation of electric signals observed in the Ioannina region (Greece), *C.R. Acad. Sci. Paris*, *320*, part IIa, 547-554, 1995.

Honkura, Y., Electric fields in the conducting crust for oscillating electric dipole sources, in *Proceedings of the International Workshop on Low-Frequency Electrical Precursors*, Rep. 92-15, edited by S. K. Park, , Inst. of Geophys. and Planet. Phys., Univ. of Calif., Riverside, 1992.

Hunter, R. J., *Zeta Potential in Colloid Science*, Academic, San Diego, Calif., 1981.

Ishido, T., and H. Mizutani, Experimental and theoretical basis of electrokinetic phenomena in rock-water systems and its applications to geophysics, *J. Geophys. Res.*, *86*, 1763-1775, 1981.

Jin, A., Some results of observations and studies on Earth resistivity in China (abstract), *Eos Trans. AGU*, *66*(46), 1066-1067, 1985.

Jouniaux, L., and J.-P. Pozzi, Streaming potential and permeability of saturated sandstones under triaxial stress: Consequences for electrotelluric anomalies prior to earthquakes, *J. Geophys. Res.*, *100*, 10,197-10,209, 1995a.

Jouniaux, L., and J.-P. Pozzi, Permeability dependence of streaming potential in rocks for various fluid conductivities, *Geophys. Res. Lett.*, *22*, 485-488, 1995b.

Jouniaux, L., S. Lallemant, and J.-P. Pozzi, Changes in the permeability, streaming potential and resistivity of a claystone from the Nankai prism under stress, *Geophys. Res. Lett.*, *21*, 149-152, 1994.

King, C.-Y., N. Koizumi, and Y. Kitagawa, Hydrogeochemical anomalies and the 1995 Kobe earthquake, *Science*, *269*, 38-39, 1995.

Li, H. C., and P. L. De Bruyn, Electrokinetic and adsorption studies on quartz, *Surf.Sci.*, *5*, 203-220, 1966.

Massenet, F., and P. Van Ngoc, Experimental and theoretical basis of self-potential phenomena in volcanic areas with reference to results obtained on Mount Etna, *Earth Planet. Sci. Lett.*, *73*, 415-429, 1985.

Middleton, M. F., The relationship of streaming potential and applied pressure to pore geometry (abstract) *Ann. Geophys. Eur. Geophys. Soc.*, 178, 1996.

Miyakoshi, J., Anomalous time variation of the self-potential in the fractured zone of an active fault preceding the earthquake occurrence, *J. Geomagn. Geoelectr.*, *38*, 1015-1030, 1986.

Mizutani, H., and T. Ishido, A new interpretation of magnetic field variation associated with Matsushiro earthquake, *J. Geomagn. Geoelectr.*, *28*, 179-188, 1976.

Mizutani, H., T. Ishido, T. Yokokura, and S. Ohnishi, Electrokinetic phenomena associated with earthquakes, *Geophys. Res. Lett.*, *3*, 365-368, 1976.

Molchanov, O. A., Y. A., Kopytenko, P. M., Voronov, E. A. Kopytenko, T.G. Matiashvili, A. C. Fraser-Smith, and A. Bernadi, Results of ULF magnetic field measurements near the epicenters of the Spitak (Ms = 6.9) and Loma Prieta (Ms = 7.1) earthquakes: Comparative analysis, *Geophys. Res. Lett.*, *19*, 1495-1498, 1992.

Morat, P., J.-L. Le Mouël, G. Nover, and G. Will, Annual variation of the water saturation of a highly porous rock driven by a seasonal temperature variation and measured by an array of electrodes, *C. R. Acad. Sci. Paris*, *315*, Ser. II, 1083-1090, 1992.

Morgan, F. D., E. R. Williams, and T. R. Madden, Streaming potential properties of Westerly granite with applications, *J. Geophys. Res.*, *94*, 12,449-12,461, 1989.

Muir-Wood, R., and G. C. P. King, Hydrological signatures of earthquake strain, *J. Geophys. Res.*, *98*, 22,035-22,068, 1993.

Murakami, H., H. Mizutani, and S. Nabetani, Self-potential anomalies associated with an active fault, *J. Geomagn. Geoelectr.*, *36*, 351-376, 1984.

Myachkin, V.I., G.A. Sobolev, N.A. Dolbilkina, V.N. Morozow, and V.B. Preobrazensky, The study of variations in geophysical fields near focal zones of Kamchatka, *Tectonophysics*, *14*, 287-293, 1972.

Nourbehecht, B., Irreversible thermodynamic effects in inhomogeneous media and their applications in certain geoelectric problems, Ph.D., thesis, Mass. Inst. of Technol., Cambridge, 1963.

Nur, A., Dilatancy, pore fluids, and premonitory variations of ts/tp travel times, *Bull. Seismol. Soc. Am.*, *62*, 1217-1222, 1972.

Overbeek, J. T. G., Electrochemistry of the double layer, in *Colloid Science*, vol. 1, *Irreversible Systems*, edited by H. R. Kruyt, pp.115-193, Elsevier, New York, 1952.

Pozzi, J.-P., and L. Jouniaux, Electrical effects of fluid circulation in sediments and seismic prediction, *C. R. Acad. Sci. Paris*, *318*, Ser. II, 73-77, 1994.

Pride, S.R., Governing equations for the coupled electromagnetics and acoustics of porous media, *Phys. Rev. B*, *50*, 15,678-15,696, 1994.

Pride, S.R., and F.D. Morgan, Electrokinetic dissipation induced by seismic waves, *Geophysics*, *56*, 914-925, 1991.

Revil, A., M. Darot, and P.A. Pezard, From surface electrical properties to

spontaneous potentials in porous media, *Surv. Geophys., 17,* 331-346, 1996.

Roeloffs, E. A., S. S. Burford, F.S. Riley, and A.W. Records, Hydrologic effects on water level changes associated with episodic fault creep near Parkfield, California, *J. Geophys. Res., 94,* 12,387-12,402, 1989.

Ruffet, C., La conductivité électrique complexe dans quelques roches crustales, PhD. Thesis, Université Strasbourg I, 1993.

Ruffet, C., Y. Gueguen, and M. Darot, Complex conductivity measurements and fractal nature of porosity, *Geophysics, 56,* (6), 758-768, 1991.

Scholz, C. H., L. R. Sykes, and Y. P. Aggrawal, Earthquake prediction : A physical basis, *Science, 181,* 803-810, 1973.

Serebryakova, O. N., S. V. Bilichenko, V. M. Chmyrev, M. Parrot, J. L. Rauch, F. Lefeuvre, and O. A. Pokhotelov, Electromagnetic ELF radiation from earthquake regions as observed by low-altitude satellites, *Geophys. Res. Lett., 19,* 91-94, 1992.

Sharma, M. M., J.F. Kuo, and T. F. Yen, Further investigation of the surface charge properties of oxide surfaces in oil-bearing sands and sandstones, *J. Colloid Interface Sci., 115,* 9-16, 1987.

Sobolev, G. A., Application of electric method to the tentative short-term forecast of Kamchatka earthquakes, *Pure Appl. Geophys., 113,* 229-235, 1975.

Somasundaran, P. and R..D. Kulkarni, A new streaming potential apparatus and study of temperature effects using it, *J. Colloid Interface Sci., 45,* 591-600, 1973.

Stern, O., Zür theorie der electrolytischen doppelschicht, *Z. Elecktrochem., 30,* 508-516, 1924.

Toutain, J.-P., M. Munoz, F. Poitrasson, and A.C. Lienard, Springwater chloride ion anomaly prior to a Ml=5.2 pyrenean earthquake, , *Earth Planet. Sci. Lett.,* in press, 1997.

Tsunogai, U. and H. Wakita, Precursory chemical changes in ground water: Kobe earthquake, Japan, *Science, 269,* 61-63, 1995.

Varotsos, P., and K. Alexopoulos, Physical properties of the variations of the electric field of the Earth preceding earthquakes, I, *Tectonophysics, 110,* 73-98, 1984a.

Varotsos, P., and K. Alexopoulos, Physical properties of the variations of the electric field of the Earth preceding earthquakes, II, Determination of epicenter and magnitude, *Tectonophysics, 110,* 99-125, 1984b.

Wakita, H., Changes in groundwater level and chemical composition, in *Earthquake Prediction Techniques,* edited by T. Asada, pp. 175-216, Univ. of Tokyo Press, Tokyo, 1982.

L. Jouniaux and J.-P. Pozzi, Laboratoire de Géologie de l'École Normale Supérieure , URA 1316 du CNRS, 24, rue Lhomond, 75231 Paris Cédex 05, France. (e-mail: jouniaux@magnetit.ens.fr; pozzi@magnetit.ens.fr)